Investigation of Geant4 Simulation of Electron Backscattering

Tullio Basaglia, Min Cheol Han, Gabriela Hoff, Chan Hyeong Kim, Sung Hun Kim, Maria Grazia Pia, and Paolo Saracco

***Abstract*—A test of Geant4 simulation of electron backscattering recently published in this journal prompted further investigation into the causes of the observed behaviour. An interplay between features of geometry and physics algorithms implemented in Geant4 is found to significantly affect the accuracy of backscattering simulation in some physics configurations.**

***Index Terms*—Electrons, Geant4, Monte Carlo, simulation.**

I. Introduction

THE simulation of electron backscattering is a sensitive testing ground to appraise the capabilities of a Monte Carlo transport code. A recent paper [1] evaluated the simulation of the electron backscattering fraction based on Geant4 [2], [3] with respect to a large sample of experimental data collected from the literature. The statistical analysis comparing simulated and experimental data identified significant differences in accuracy associated with different Geant4 multiple scattering models, including those instantiated in predefined electromagnetic *PhysicsConstructor* classes intended to facilitate the physics configuration of user applications. It also highlighted inconsistencies in the behaviour of the Urban multiple scattering model in association with some of its optional settings.

The outcome of the validation tests reported in [1] prompted further investigations to elucidate the origin of the observed behaviour. This paper documents the results of this delving; they constitute the grounds for further improvements to Geant4, and a reference point for the experimental community regarding simulation scenarios that could be prone to similar shortcomings when using the Geant4 versions considered in this test.

The physics context, simulation environment and analysis methods pertinent to this paper are the same as in [1], where they are extensively described. They are only briefly summarized in the following sections to facilitate the appraisal of the results reported here; further details can be found in [1].

Manuscript received March 30, 2015; revised May 31, 2015; accepted June 03, 2015. Date of publication July 17, 2015; date of current version August 14, 2015.

T. Basaglia is with CERN, CH-1211 Genève 23, Switzerland (e-mail: Tullio.Basaglia@cern.ch).

G. Hoff is with the CAPES Foundation, Ministry of Education of Brazil, Brasilia–DF 70040-020, Brazil (e-mail: ghoff.gesic@gmail.com).

M. C. Han, C. H. Kim, and S. H. Kim are with the Department of Nuclear Engineering, Hanyang University, Seoul 133-791, Korea (e-mail: ksh4249@hanyang.ac.kr; mchan@hanyang.ac.kr; chkim@hanyang.ac.kr).

M. G. Pia and P. Saracco are with INFN Sezione di Genova, I-16146 Genova, Italy (e-mail: MariaGrazia.Pia@ge.infn.it; Paolo.Saracco@ge.infn.it).

Color versions of one or more of the figures in this paper are available online at http://ieeexplore.ieee.org.

Digital Object Identifier 10.1109/TNS.2015.2442292

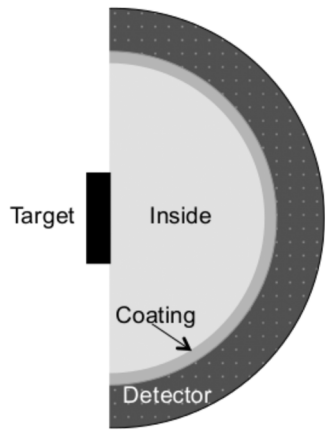

Fig. 1. Longitudinal sketch of the geometrical elements involved in the simulation: the target volume (black), the detector volume (dotted dark grey), the inner coating of the detector (medium grey) and the cavity volume in the backward hemisphere (light grey), identified as "Inside". The figure is not to scale to facilitate the visibility of all the components of the experimental setup.

II. Simulation Features

A. Overview of the Simulation Configuration

The simulation concerns the estimate of the fraction of electrons that are backscattered from a semi-infinite or infinite target of pure elemental composition.

For each test case associated with a measurement, the configuration of the simulation application reproduces the essential characteristics of the experimental setup reported in the literature. The test cases are the same as in [1].

The geometrical configuration of the simulation is schematically illustrated in Fig. 1. The target is modelled as a parallelepiped or a disk (an instance of the *G4Box* and *G4Tubs* classes, respectively), consistent with the shape, size and material composition documented in the experimental reference corresponding to each test case. Backscattered electrons are detected when entering a sensitive volume consisting of a hemispherical shell, identified as "Detector" in Fig. 1. The detector is complemented by an inner coating layer, which some reference papers report to be part of the experimental setup. The coating material can be optionally defined as equivalent to galactic vacuum to mimic experimental configurations not explicitly documenting the presence of a coating layer. The cavity

TABLE I
MULTIPLE SCATTERING CONFIGURATIONS EVALUATED IN THIS INVESTIGATION OF ELECTRON BACKSCATTERING SIMULATION

Configuration	Description	Process class	Model class	StepLimitType	RangeFactor
Urban	Urban model, user step limit	G4eMultipleScattering	G4UrbanMscModel	default	default
UrbanB	Urban model, user step limit	G4eMultipleScattering	G4UrbanMscModel	DistanceToBoundary	default
UrbanBRF	Urban model	G4eMultipleScattering	G4UrbanMscModel	DistanceToBoundary	0.01
GSBRF	Goudsmit-Saunderson	G4eMultipleScattering	G4GoudsmitSaundersonModel	DistanceToBoundary	0.01
WentzelBRF	WentzelVI model	G4eMultipleScattering	G4WentzelVIModel	DistanceToBoundary	0.01
		PhysicsConstructor class			
EmLivermore		G4EmLivermorePhysics		DistanceToBoundary	0.01
EmStd	Predefined	G4EmStandardPhysics		default	default
EmOpt1	electromagnetic	G4EmStandardPhysics_option1		default	default
EmOpt2	physics	G4EmStandardPhysics_option2		default	default
EmOpt3	selections	G4EmStandardPhysics_option3		DistanceToBoundary	default
EmOpt4		G4EmStandardPhysics_option4		DistanceToBoundary *(10.0)* SafetyPlus *(10.1)*	0.01 *(10.0)* 0.02 *(10.1)*

internal to the detector and coating layer, identified in Fig. 1 as "Inside", is a hemispherical volume filled by default with low density material equivalent to galactic vacuum or other gaseous material to reflect the experimental configurations documented in the literature. The Detector, Coating and Inside volumes are modelled as instances of the Geant4 *G4Sphere* class. The target and backward detection system are placed in an overall enclosing volume, identified in Geant4 terms as the "World". The entrance face of the target is placed in the computational world at Z coordinate equal to zero; the centres of the Inside, Detector and Coating spheres coincide with the centre of the computational world at coordinates (0,0,0).

The correctness of the geometrical configuration of the simulation has been verified by means of two test methods provided by Geant4 [17] to identify malformed geometries, that is overlapping volumes: at the time of construction, by activating the optional built-in ability of the *G4PVPlacement* constructor to detect overlaps of placed volumes when instantiating a placement, and at run-time, by using built-in Geant4 commands that activate verification tests for the user-defined geometry. The latter consisted of a Geant4 "*line_test*", which shot lines perpendicular to the target face forwards and backwards to detect possible overlaps, traversing recursively all the volumes present in the geometrical setup. These tests did not report any problem regarding the geometry model constructed in the simulation application.

The origin of primary particles is located at the centre of the computational world. Primary electrons are generated with momentum direction along the Z axis, i.e. orthogonal to the entrance face of the target; their energy is defined according to the corresponding experimental references.

The physics configuration of the simulation is extensively described in [1]. The simulation application design allows the choice of several multiple or single electron scattering modelling options (Urban [4]–[6], Goudsmit-Saunderson [7]–[9], WentzelVI [10], [11], Coulomb [12]), complemented by other electron and photon interactions modelled in Geant4 standard [13] and low energy [14]–[16] electromagnetic packages, or, alternatively, the choice of predefined electromagnetic *PhysicsConstructors* encompassed in the Geant4 *physics_lists* package [17]. In addition, it allows further selections of algorithms characterizing the treatment of electron multiple scattering, such as the methods of calculation of the step limitation, e.g. the *DistanceToBoundary* algorithm and the so-called *range factor* parameter.

B. Configurations in this Investigation

The study reported in this paper investigated possible effects on the simulated electron backscattering fraction related to the geometrical configuration of the experimental setup. For this purpose, some features of the experimental model described in Section II-A were modified: the position of the target, which was displaced along the Z axis with respect to the backward detection system, the construction of the backward system as a hierarchy of volumes rather than as volumes individually placed in the World, and the origin of primary electrons.

The investigation focused on a subset of the multiple scattering configurations examined in [1]: they are listed in Table I, where version numbers in parentheses identify different settings in the course of the evolution of the Geant4 toolkit. The treatment of other electron and photon interactions was based on the EEDL (Evaluated Electron Data Library) [18] and EPDL (Evaluated Photon Data Library) [19] data libraries in the simulation configurations involving the selection of specific multiple scattering models. Configurations involving predefined electromagnetic *PhysicsConstructor* classes handle electron and photon interactions according to the settings implemented in those classes [17]. A limited set of simulations involved the Coulomb single scattering model. Further details about the features of these physics configurations can be found in [1] and in the associated references cited therein.

The simulation production for this investigation was performed under the same conditions as that described in [1].

III. DATA ANALYSIS

The fraction of backscattered electrons calculated by the simulation is compared with measurements by means of statistical methods. The compatibility between simulated and experimental data is established by goodness-of-fit tests. The significance level of the tests is set at 0.01. Four goodness-of-fit tests (the Anderson-Darling (AD) [20], [21], Cramer-von Mises (CvM) [22], [23], Kolmogorov-Smirnov (KS) [24], [25] and Watson [26] tests) are applied to mitigate the risk of introducing systematic effects in the results of the analysis due

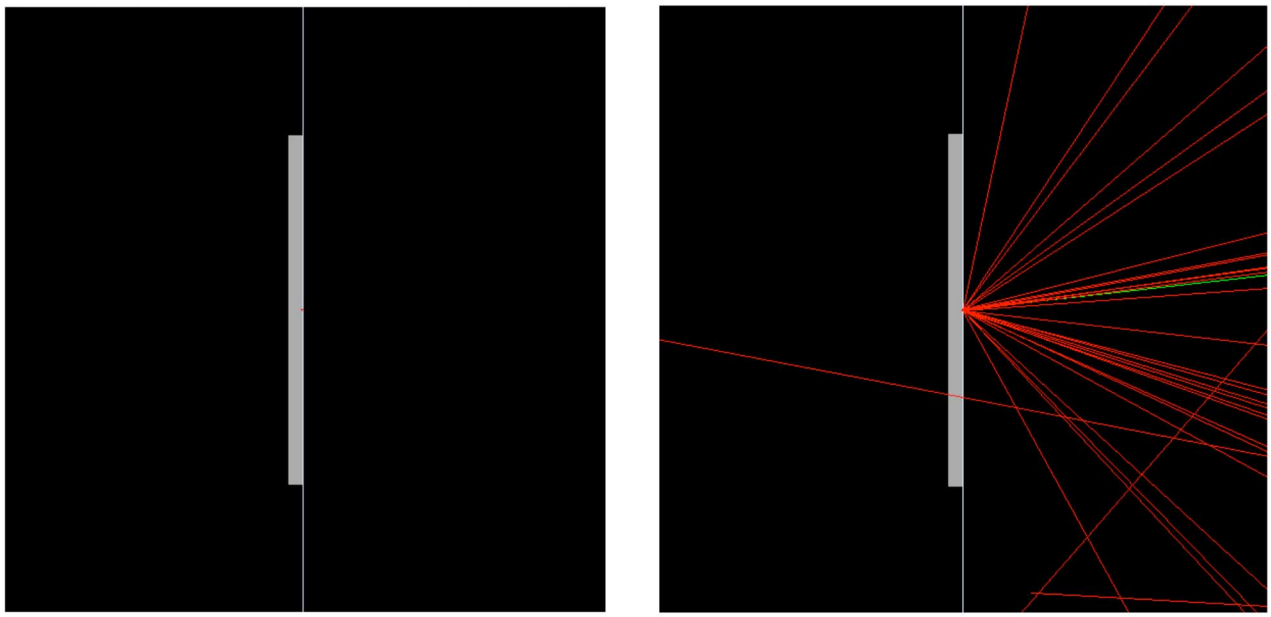

Fig. 2. Visualization of 200 simulated events, concerning 100 keV electrons impinging on a silicon target (appearing as a grey rectangle) with a physics configuration based on the G4EmStandardPhysics_option3 PhysicsConstructor in Geant4 10.1. (a) The image on the left corresponds to the original simulation setup: no backscattered electrons are visible. (b) The image on the right was obtained displacing the target by 1 pm along the Z axis: backscattered electrons are visible as red tracks; green lines represent photons. (a) Original geometry setup. (b) Geometry setup with the target displaced by 1 pm.

to peculiarities of the mathematical formulations of the tests. Compatibility with experimental data of a given simulation configuration is summarized by means of a variable named "efficiency", which represents the fraction of test cases where the p-value resulting from goodness-of-fit tests is larger than the predefined significance level.

The data analysis uses the Statistical Toolkit [27], [28] and R [29]. Further details, along with extensive discussion of the methodology applied in the validation tests of Geant4 simulation, can be found in [1].

IV. Results

A. Effects of Step Limitation Algorithms

A noticeable feature observed in the outcome of goodness-of-fit tests reported in Table VII of [1] is that multiple scattering configurations that encompass algorithms of step limitation explicitly involving the distance from geometrical boundaries exhibit significantly lower efficiencies in Geant4 versions later than 9.2 with respect to similar configurations. This is the case, for instance, for the UrbanB configuration with respect to the Urban one in Geant4 versions 9.3 to 9.6, and for the G4EmStandardPhysics_option3 and G4EmStandardPhysics_option4 configurations with respect to G4EmStandardPhysics_option1 and G4EmStandardPhysics_option2 in Geant4 versions 9.6 to 10.1. This observation hints at some interplay between Geant4 multiple scattering settings involving algorithms related to geometrical boundaries and the way Geant4 kernel handles the geometrical model of the backscattering experiments.

In the geometrical configuration of the backscattering test a relevant geometrical boundary is the surface of the target volume placed at Z equal to zero, which is traversed by backscattered electrons. Although neither the construction-time nor the run-time test of the simulation geometry identified any anomalies regarding overlaps of the target with other volumes, in particular with the adjacent "Inside" volume, a test was devised to investigate whether any algorithmic feature in Geant4 kernel could interfere with the target boundaries, specifically the one relevant to backscattering. For this purpose, the target was slightly displaced in the forward Z direction, in such a way that it was no longer adjacent to the "Inside" volume. This displacement introduced a small gap in the geometrical acceptance of the detector, which no longer covered the whole solid angle where backscattered electrons should be counted. Nevertheless, if the target displacement is small, the loss in detection acceptance is also small.

It was found that this modification of the geometrical setup of the experiment has significant effects on the outcome of the simulation for displacement of the target larger than 0.5 pm. This numerical value corresponds to half the nominal thickness (1 pm) of an artificial "surface" implicitly associated with Geant4 volumes [30], known as "tolerance".

The apparent suppression of electron backscattering in configurations involving "DistanceToBoundary" step limitation, and the generation of backscattered electrons, when the target is displaced along the Z axis, are clearly visible with Geant4 graphical visualization tools, independently from algorithms counting electrons entering the detector and the use of Geant4 functionality for defining sensitive detectors and scoring hits in them. As an example, Fig. 2 displays the result of 200 events accumulated over the same scene, resulting from the interactions of 100 keV electrons impinging on a silicon target. The simulation involves the G4EmStandardPhysics_option3 PhysicsConstructor in Geant4 10.1, which encompasses

TABLE II
EFFICIENCY OF PHYSICS CONFIGURATIONS WITH GEANT4 VERSIONS 9.1 TO 10.1 FOR DIFFERENT ΔZ DISPLACEMENTS OF THE TARGET AND OF THE PRIMARY ELECTRON SOURCE

Physics	Geant4	1-20 keV			20-100 keV			$> 100keV$		
configuration	version	ΔZ=0	ΔZ_{target}=1 pm	ΔZ_{source}=1 pm	ΔZ=0	ΔZ_{target}=1 pm	ΔZ_{source}=1 pm	ΔZ=0	ΔZ_{target}=1 pm	ΔZ_{source}=1 pm
Urban	9.1	< 0.01	0.11±0.03	0.07±0.02	0.10±0.03	0.23±0.04	0.24±0.04	0.79±0.05	0.72±0.06	0.82±0.05
Urban	9.2	< 0.01	0.07±0.02	0.03±0.02	0.03±0.02	0.07±0.03	0.08±0.03	0.79±0.05	0.82±0.05	0.79±0.05
Urban	9.3	< 0.01	0.04±0.02	0.02±0.01	0.09±0.03	0.08±0.03	0.08±0.03	0.74±0.06	0.72±0.06	0.70±0.06
Urban	9.4	< 0.01	0.05±0.02	0.03±0.02	0.10±0.03	0.12±0.03	0.08±0.03	0.56±0.06	0.60±0.06	0.56±0.07
Urban	9.6	< 0.01	0.10±0.02	0.09±0.03	0.17±0.04	0.20±0.04	0.20±0.04	0.68±0.06	0.74±0.06	0.68±0.06
Urban	10.0	< 0.01	0.08±0.02	0.07±0.02	< 0.01	0.21±0.04	0.17±0.04	0.11±0.04	0.63±0.06	0.63±0.06
Urban	10.1	< 0.01	0.08±0.02	0.07±0.02	< 0.01	0.22±0.04	0.21±0.04	0.07±0.04	0.63±0.06	0.61±0.06
UrbanB	9.1	< 0.01	0.11±0.03	0.07±0.02	0.10±0.02	0.23±0.04	0.24±0.04	0.79±0.05	0.72±0.06	0.82±0.05
UrbanB	9.2	< 0.01	0.07±0.02	0.03±0.02	0.03±0.02	0.07±0.02	0.08±0.03	0.79±0.05	0.82±0.05	0.79±0.05
UrbanB	9.3	< 0.01	0.06±0.02	0.04±0.02	< 0.01	0.07±0.02	0.07±0.02	0.11±0.04	0.74±0.06	0.72±0.06
UrbanB	9.4	< 0.01	0.06±0.02	0.02±0.01	< 0.01	0.07±0.02	0.10±0.03	0.07±0.04	0.61±0.06	0.60±0.06
UrbanB	9.6	< 0.01	0.09±0.02	0.07±0.02	< 0.01	0.17±0.04	0.16±0.03	0.05±0.03	0.67±0.06	0.65±0.06
UrbanB	10.0	< 0.01	0.07±0.02	0.04±0.02	< 0.01	0.18±0.04	0.20±0.04	0.07±0.04	0.63±0.06	0.60±0.06
UrbanB	10.1	< 0.01	0.07±0.02	0.04±0.02	< 0.01	0.19±0.04	0.18±0.04	0.09±0.04	0.61±0.06	0.68±0.06
UrbanBRF	9.1	< 0.01	-	-	< 0.01	-	-	0.05±0.03	-	-
UrbanBRF	9.2	< 0.01	0.04±0.02	0.02±0.01	< 0.01	0.05±0.02	0.04±0.02	0.02±0.02	0.54±0.06	0.58±0.07
UrbanBRF	9.3	< 0.01	0.07±0.02	0.04±0.02	< 0.01	0.16±0.03	0.17±0.04	0.07±0.04	0.58±0.06	0.60±0.06
UrbanBRF	9.4	< 0.01	0.07±0.02	0.06±0.02	< 0.01	0.16±0.03	0.13±0.03	0.07±0.04	0.60±0.06	0.61±0.06
UrbanBRF	9.6	< 0.01	0.15±0.03	0.16±0.03	< 0.01	0.21±0.04	0.23±0.04	0.07±0.04	0.75±0.06	0.72±0.06
UrbanBRF	10.0	< 0.01	0.10±0.03	0.08±0.02	< 0.01	0.30±0.04	0.32±0.04	0.07±0.04	0.54±0.06	0.56±0.07
UrbanBRF	10.1	< 0.01	0.10±0.03	0.08±0.02	< 0.01	0.25±0.04	0.27±0.04	0.09±0.04	0.61±0.06	0.63±0.06
GSBRF	9.3	< 0.01	0.07±0.02	0.04±0.02	< 0.01	0.21±0.04	0.17±0.04	0.07±0.03	0.58±0.06	0.58±0.06
GSBRF	9.4	< 0.01	0.07±0.02	0.06±0.02	< 0.01	0.16±0.03	0.13±0.03	0.07±0.03	0.60±0.06	0.61±0.06
GSBRF	9.6	< 0.01	0.32±0.04	0.37±0.04	0.01±0.01	0.54±0.05	0.54±0.05	0.58±0.06	0.96±0.02	0.95±0.03
GSBRF	10.0	< 0.01	0.34±0.04	0.40±0.04	0.01±0.01	0.54±0.05	0.52±0.05	0.58±0.06	0.95±0.03	0.95±0.03
GSBRF	10.1	< 0.01	0.26±0.04	0.24±0.04	0.01±0.01	0.01±0.01	0.01±0.01	0.39±0.06	0.46±0.06	0.46±0.07
WentzelBRF	9.3	0.18±0.03	0.08±0.02	0.10±0.03	0.09±0.03	< 0.01	< 0.01	0.60±0.06	0.19±0.05	0.19±0.05
WentzelBRF	9.4	0.02±0.01	0.51±0.04	0.52±0.05	0.21±0.04	< 0.01	< 0.01	0.61±0.06	0.07±0.04	0.07±0.03
WentzelBRF	9.6	0.46±0.04	0.48±0.04	0.46±0.04	0.44±0.05	0.43±0.05	0.48±0.05	0.79±0.05	0.74±0.06	0.72±0.06
WentzelBRF	10.0	0.49±0.04	0.50±0.04	0.47±0.05	0.44±0.05	0.44±0.05	0.50±0.05	0.81±0.05	0.81±0.05	0.77±0.06
WentzelBRF	10.1	< 0.01	0.26±0.04	0.28±0.04	0.01±0.01	0.15±0.03	0.14±0.03	0.42±0.06	0.75±0.06	0.75±0.06
EmLivermore	9.6	< 0.01	0.10±0.03	0.10±0.03	< 0.01	0.24±0.04	0.25±0.04	0.07±0.04	0.65±0.06	0.67±0.06
EmLivermore	10.0	< 0.01	0.10±0.03	0.08±0.02	< 0.01	0.27±0.04	0.30±0.04	0.05±0.03	0.63±0.06	0.65±0.06
EmLivermore	10.1	< 0.01	0.10±0.03	0.08±0.02	< 0.01	0.24±0.04	0.24±0.04	0.07±0.04	0.68±0.06	0.65±0.06
EmStd	9.6	< 0.01	0.18±0.03	0.19±0.04	< 0.01	0.18±0.04	0.20±0.04	0.40±0.06	0.74±0.05	0.75±0.06
EmStd	10.0	< 0.01	0.13±0.03	0.12±0.03	< 0.01	0.21±0.04	0.21±0.04	0.07±0.04	0.70±0.05	0.67±0.06
EmStd	10.1	< 0.01	0.13±0.03	0.12±0.03	< 0.01	0.17±0.04	0.18±0.04	0.05±0.03	0.72±0.05	0.70±0.06
EmOpt1	9.6	< 0.01	< 0.01	< 0.01	< 0.01	< 0.01	< 0.01	0.33±0.06	0.37±0.06	0.39±0.05
EmOpt1	10.0	< 0.01	0.01±0.01	< 0.01	< 0.01	< 0.01	< 0.01	0.39±0.06	0.35±0.06	0.39±0.05
EmOpt1	10.1	< 0.01	0.02±0.01	< 0.01	< 0.01	< 0.01	< 0.01	0.14±0.05	0.39±0.06	0.39±0.05
EmOpt2	9.6	< 0.01	< 0.01	< 0.01	< 0.01	< 0.01	< 0.01	0.32±0.06	0.37±0.05	0.39±0.05
EmOpt2	10.0	< 0.01	0.01±0.01	< 0.01	< 0.01	< 0.01	< 0.01	0.37±0.06	0.39±0.05	0.39±0.05
EmOpt2	10.1	< 0.01	0.02±0.01	< 0.01	< 0.01	< 0.01	< 0.01	0.16±0.05	0.39±0.05	0.39±0.05
EmOpt3	9.6	< 0.01	0.25±0.04	0.27±0.03	< 0.01	0.28±0.04	0.29±0.04	0.07±0.04	0.77±0.04	0.74±0.06
EmOpt3	10.0	< 0.01	0.13±0.03	0.12±0.03	< 0.01	0.13±0.03	0.13±0.03	0.07±0.04	0.68±0.04	0.70±0.06
EmOpt3	10.1	< 0.01	0.13±0.03	0.13±0.03	< 0.01	0.13±0.03	0.11±0.03	0.07±0.04	0.70±0.04	0.70±0.06
EmOpt4	9.6	< 0.01	0.10±0.03	0.07±0.02	< 0.01	0.27±0.04	0.24±0.04	0.07±0.04	0.68±0.06	0.68±0.06
EmOpt4	10.0	< 0.01	0.10±0.03	0.08±0.02	< 0.01	0.29±0.04	0.27±0.04	0.09±0.04	0.68±0.06	0.68±0.06
EmOpt4	10.1	*< 0.01*	*< 0.01*	0.15±0.03	*< 0.01*	*0.22±0.04*	0.24±0.04	*< 0.02*	*0.30±0.06*	0.79±0.05
Coulomb	10.0	0.49±0.04	0.50±0.05	-	0.40±0.05	0.46±0.05	-	0.79±0.05	0.81±0.05	-
Coulomb	10.1	< 0.01	< 0.01	-	< 0.01	< 0.01	-	< 0.02	< 0.02	-

"DistanceToBoundary" step limitation in multiple scattering simulation. No backscattered electrons are visible in the original geometrical configuration, while they are abundantly generated when the target is displaced by 1 pm along the *Z* axis. Extensive documentation of the simulation behaviour through event displays in several configurations is avalable in [31].

The efficiency of the physics configurations considered in this investigation is reported in Table II for the original geometrical configuration and for a configuration where the target is displaced by 1 pm in the forward direction. For convenience, only efficiencies based on the outcome of the Anderson-Darling test are listed, given the similarity of the results of different goodness-of-fit tests discussed in [1]. The results are grouped in three energy ranges as in [1]. Values for the UrbanBRF configuration with Geant4 version 9.1 are not listed, since the simulation of a few test cases could not be completed due to excessive consumption of computational resources.

Statistically significant effects of the target displacement are visible in the results of the Urban multiple scattering model of Geant4 versions 9.3 to 9.6, when a step limitation algorithm explicitly involving volume boundaries (as in UrbanB and UrbanBRF configurations) is selected. An example of the backscattering fraction simulated with the original geometrical setup and with a modified setup, where the target has been displaced by 1 pm along the *Z* axis, is shown in Fig. 3, concerning the UrbanB physics configuration. When the target is displaced, i.e. it no longer shares the relevant boundary with the "Inside" volume, the efficiency at reproducing experimental measurement is comparable for the three settings of the Urban model, while in the original geometrical setup backscattering was suppressed in the UrbanB and UrbanBRF configurations.

Sensitivity to the displacement of the target is also visible with the GSBRF configuration of the Goudsmit-Saunderson model, which is associated with "DistanceToBoundary"

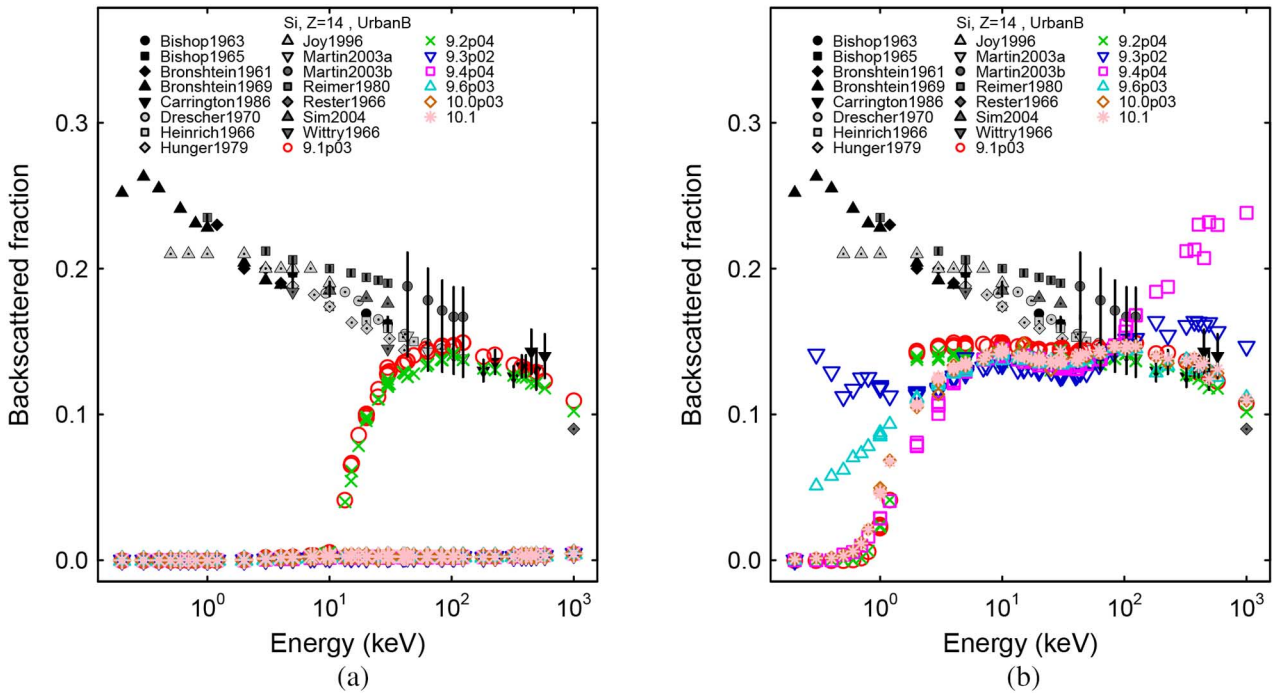

Fig. 3. Fraction of electrons backscattered from a silicon target as a function of the electron beam energy, obtained with the target adjacent to the backward hemisphere (left) and with the target displaced along the Z axis (right): experimental data (black and grey filled symbols) and simulation results (empty symbols) with the UrbanB multiple scattering configuration in Geant4 version 9.1 (red circles), 9.2 (green crosses), 9.3 (blue upside down triangles), 9.4 (magenta squares), 9.6 (turquoise triangles), 10.0 (brown diamonds) and 10.1 (pink asterisks). The plot on the left corresponds to the original configuration, while the plot on the right was obtained displacing the target by 1 pm. (a) Geometry setup with target adjacent to the backward hemisphere. (b) Geometry setup with displaced target.

step limitation. Detailed comments concerning the Geant4 Goudsmit-Saunderson model are in Section IV-D.

Consistently, the results of predefined electromagnetic constructors G4EmStandardPhysics_option3, G4EmStandardPhysics_option4 and G4EmLivermorePhysics, which enforce "DistanceToBoundary" step limitation, are sensitive to the displacement of the target, while those of G4EmStandardPhysics_option1 and G4EmStandardPhysics_option2, which use a "Minimal" algorithm for step limitation in multiple scattering, are not. This statement does not apply to G4EmStandardPhysics_option4 in Geant4 version 10.1, which adopts a new "SafetyPlus" algorithm that generates some anomalous error messages in the course of the simulation. Therefore the efficiency associated with this configuration in Geant4 10.1, listed in italic in Table II, should not be considered in the evaluation of the evolution of its performance.

These findings hint at the introduction of some dependency on geometrical features in algorithms related to electron multiple scattering, starting with Geant4 version 9.3.

In this context it is worth remarking that the multiple scattering algorithm originally implemented in Geant4 did not restrict the step size [32], [33]. Step limitation by multiple scattering was introduced at a later stage [6]. The step limitation algorithms implemented in Geant4 are of empirical nature: they are not directly related to the theoretical foundations of the models of electron multiple scattering. The parameters they embed and the criteria they implement usually derive from a calibration process, in which they were adjusted to reproduce a small set of experimental benchmarks.

The effects of the target displacement in test cases involving the WentzelVI multiple scattering model are ambiguous: in later Geant4 versions they are consistent with the previous remarks, while in earlier versions the target displacement is associated with lower efficiency at reproducing experimental data. Nevertheless, the WentzelVI multiple scattering model de facto incorporates the treatment of single scattering as in the Geant4 Coulomb scattering model: so one should not necessarily expect algorithms concerning single scattering to behave similarly to those associated with proper multiple scattering models, such as Urban and Goudsmit-Saunderson.

Effects of the target displacement are visible in the efficiencies associated with the default Urban model configuration and the predefined G4EmStandardPhysics *PhysicsConstructor* of Geant4 version 10.0 and 10.1, although step limitation in multiple scattering is performed according to an algorithm using "Safety" rather than "DistanceToBoundary". We verified that the simulation based on Geant4 version 10.0 and 10.1 behaves consistently with that of Geant4 9.6, when the UrbanMscModel, instantiated by the electron multiple scattering process of these versions, is replaced by UrbanMscModel95, which was instantiated by default in version 9.6. This test hints that sensitivity to the treatment of the boundary may be embedded in portions of the code of UrbanMscModel and UrbanMscModel95 pertinent to the "Safety" step limitation option. It is also worthwhile to note that the evaluation of geometrical safety has evolved from Geant4 9.6 to later versions [34], and that this evolution was intended to address the treatment of physics effects close to volumes boundaries.

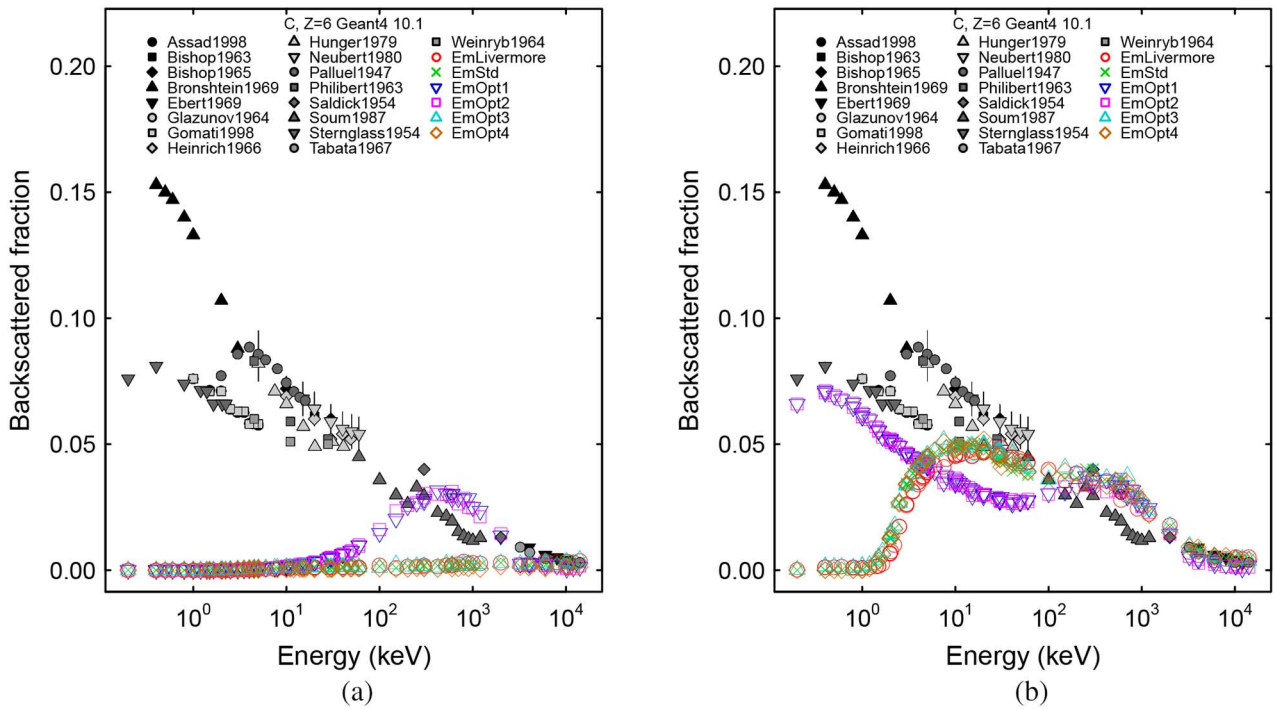

Fig. 4. Fraction of electrons backscattered from a carbon target as a function of the electron beam energy: experimental data (black and grey filled symbols) and Geant4 10.0 simulation results with G4EmLivermorePhysics (red empty circles), G4EmStandardPhysics (green crosses), G4EmStandardPhysics_option1 (blue empty upside-down triangles), G4EmStandardPhysics_option2 (magenta empty squares), G4EmStandardPhysics_option3 (turquoise empty triangles) and G4EmStandardPhysics_option4 (brown empty diamonds) PhysicsConstructors. The plot on the left corresponds to the original simulation setup, while the plot on the right was obtained displacing the primary electron source by 1 pm backwards. (a) Setup with electron source in the origin of the "World". (b) Setup with primary source moved to Z $= -1$ pm.

The performance of the Coulomb single scattering model does not appear to be affected by the displacement of the target in Geant4 versions 10.0 and 10.1. The production with Geant4 version 9.6 could not be completed over all the experimental test cases, since some jobs had to be terminated after 24 hours' running, presumably due to endless loops. This error was not observed in the production with the original geometry configuration.

B. Effects Related to the Primary Particle Source

Results similar to those for a displaced target are obtained with the original geometry configuration described in Section II-A by displacing the Z origin of primary particles by 1 pm, rather than the target: in this configuration the source is placed in the "Inside" volume, rather than being placed in the origin of the World.

The corresponding efficiencies are listed in Table II; an example, concerning simulations with predefined *PhysicsConstructors*, is illustrated in Fig. 4. No error is signaled in either positioning of the primary particle source, nor in the course of particle transport with either source configurations, even when Geant4 built-in checks of navigation through the geometry [17] were executed at tracking time setting the highest level of verbosity.

C. Effects of Different Geometrical Construction Methods

In a further investigation of the interplay between geometry and physics, the backward geometrical setup, originally consisting of two hemispherical shells and a hemisphere placed in the "World", was replaced by a hierarchy of hemispheres: in this setup the outer "Detector" hemisphere contains the "Coating" hemisphere, which in turns contains the "Inside" hemisphere. The dimensions of the geometrical components, their relative positions and material compositions were identical in both setups.

The construction-time and run-time geometry tests did not identify any anomaly in this setup either, but a warning message was issued at run-time, apparently related to the inability of Geant4 navigator, which is responsible for locating points in the geometry and computing distances to geometry boundaries, to deal with primary particles generated in the centre of the computational world. This warning message, which did not appear in the original setup, stated that particles were "pushed" by 100 pm into the target. To avoid it, the origin of primary particles was moved back by 1 pm as in the previously mentioned test configuration.

The simulation of this configuration was performed over Geant4 versions 9.6, 10.0 and 10.1 to limit the requirements of computational resources. The efficiencies at reproducing experimental data with a hierarchical geometry are statistically equivalent to the values reported in Table II for independently positioned volumes with a displaced primary particle source; they are not explicitly listed in Table II to avoid overcrowding it. The similarity of results obtained with a hierarchical geometry definition and with independent volumes placed in the "World" excludes effects on the detection of backscattered particles due to overlaps of the curved hemispherical surfaces that may have not been identified by the built-in geometry tests.

TABLE III
EFFICIENCY WITH GEANT4 GOUDSMIT-SAUNDERSON MULTIPLE SCATTERING MODEL IN TWO DIFFERENT CONFIGURATION OPTIONS, INCLUDING RESULTS FROM GEANT4 PATCHES RELEASED AFTER THE PUBLICATION OF [1]

Energy (keV)	Version	GS	GSBRF
<20	9.3p02	< 0.01	< 0.01
	9.4p04	< 0.01	< 0.01
	9.6p04	0.01 ± 0.01	< 0.01
	10.4p04	0.01 ± 0.01	< 0.01
	10.1p01	0.01 ± 0.01	< 0.01
20-100	9.3p02	0.09 ± 0.03	< 0.01
	9.4p04	0.08 ± 0.03	< 0.01
	9.6p04	0.50 ± 0.05	0.01 ± 0.01
	10.4p04	0.51 ± 0.05	0.01 ± 0.01
	10.1p01	0.50 ± 0.05	0.01 ± 0.01
>100	9.3p02	0.74 ± 0.06	0.07 ± 0.03
	9.4p04	0.58 ± 0.07	0.07 ± 0.03
	9.6p04	0.81 ± 0.05	0.58 ± 0.07
	10.4p04	0.84 ± 0.05	0.58 ± 0.07
	10.1p01	0.81 ± 0.05	0.56 ± 0.07

D. Tests with a Corrected Goudsmit-Saunderson Model

The fourth correction patches to Geant4 versions 9.6 and 10.0, identified as Geant4 version 9.6p04 and 10.0p04 respectively, were released after the submission of [1] to this journal. No significant difference was observed between the results of the backscattering test based on this version and those reported for Geant4 9.6p03 and 10.0p03, respectively, in the original geometrical setup.

The public presentation at CERN of the results of the backscattering test documented in [1], preceding the actual publication of the paper, prompted the correction of flaws, which the test contributed to identify in some Geant4 class implementations. These corrections were implemented by maintainers of Geant4 multiple scattering code other than the authors of this paper and were released in a patch to Geant4 10.1, identified as version 10.1p01.

Improved efficiency is observed with the Goudsmit-Saunderson multiple scattering model as a result of a correction included in Geant4 10.1p01, with respect to the performance documented with Geant4 10.1 in [1] and Table II in the original geometry settings.

The results concerning this model, obtained with the latest patches of all the Geant4 versions in which it is examined, are reported in Table III for two configuration options: the default configuration, identified as "GS", and the "GSBRF" configuration, which applies "DistanceToBoundary" step limitation and *RangeFactor* value similar to the UrbanBRF configuration. Due to the presence of code clones, it cannot be ascertained whether the "DistanceToBoundary" step limitation algorithms are identical, or only similar, in the GSBRF and UrbanBRF configurations.

Significant differences are observed between the GS and GSBRF configurations for energies above 20 keV. Similarly to what is reported in Section IV-A, lower compatibility with experiment is associated with "DistanceToBoundary" step limitation. These results strengthen the hypothesis of sensitivity of multiple scattering behaviour to the shared boundary surface, when the "DistanceToBoundary" algorithm is involved.

TABLE IV
EFFICIENCY WITH THE G4EMSTANDARDPHYSICS_WVI PHYSICSCONSTRUCTOR IN GEANT4 10.1 AND 10.1P01

Energy (keV)	Geant4 10.1	Geant4 10.1p01
<20	< 0.01	0.44 ± 0.04
20-100	0.01 ± 0.01	0.48 ± 0.05
>100	0.40 ± 0.06	0.79 ± 0.05

E. Performance of Modified G4EmStandardPhysics_WVI

A modification to the G4EmStandardPhysics_WVI *PhysicsConstructor* included in Geant4 10.1p01 contributed to improve the efficiency of this configuration. The results are reported in Table IV for Geant4 versions 10.1 and 10.1p01.

This *PhysicsConstructor* uses the WentzelVI model, which incorporates single Coulomb scattering modeling.

V. CONCLUSION

In-depth investigation of Geant4-based simulation of electron backscattering has highlighted an interplay between algorithms related to step limitation in electron multiple scattering and the geometrical model of backscattering experiments, which generates inconsistencies in the capability of the simulation to reproduce measurements, depending on the geometrical configuration of the experimental model. Although the geometrical configuration of the backscattering simulation had been validated by built-in Geant4 geometry checks at construction-time and at run-time, which did not detect any anomaly, the presence of an adjacent hemispherical volume affects backscattering from the target volume. This effect appears to be associated with algorithms that calculate step limitation based on "DistanceToBoundary".

The implementation of algorithms dealing with step limitation is replicated in different Geant4 multiple scattering classes: the presence of code clones, which are a known source of software maintenance issues [35], could explain some observed differences in their behaviour and evolution.

In general, the efficiency at reproducing experimental backscattering measurements increases when the target volume is displaced by a distance larger than half the size of the so-called "tolerance", i.e. the thickness of a fictitious surface associated with Geant4 volumes.

The investigation of possible effects related to the position of the primary particle source hints at navigation algorithms playing a role in the observed simulation outcome, when adjacent volumes are present. Consistent simulation results deriving from primary particle sources located at a geometrical boundary or in its proximity would be desirable, as both locations may correspond to realistic user requirements.

Simulation configurations involving adjacent volumes, which are common scenarios in experimental practice (e.g. segmented detectors, voxel models) and are validated by Geant4 built-in geometry tests, could be sensitive to effects related to electron backscattering, which in turn can affect the spatial pattern of energy deposition [1]. Experimental applications involving such

scenarios may want to check the sensitivity of their observables to the presence of adjacent volumes. Small displacements of size comparable to Geant4 "tolerance" may be a viable solution, if compatible with the requirements of the simulation.

The investigation documented in this paper suggests that Geant4 multiple scattering implementations would benefit from consistent behaviour of different algorithms related to step limitation, especially regarding their interaction with the geometry. Improvements to the software design of the Geant4 multiple scattering domain would contribute to increased transparency of the basis for its physics modelling and better understanding its operation, which are only succinctly documented at the present time.

Improved capability of reproducing experimental measurements is observed with corrected versions of the Goudsmit-Saunderson multiple scattering model and of the G4EmStandardPhysics_WVI *PhysicsConstructor* released in Geant4 10.1p01, which were motivated by the results reported in [1]. Nevertheless, the observed inconsistency of the efficiency at reproducing experimental backscattering data, depending on the configuration of the experimental setup, precludes a univocal quantification of the accuracy of Geant4 multiple scattering models and their relative comparison at the present stage. Quantification of the physics performance of these models will be meaningful once the interplay between Geant4 geometrical settings, primary source positioning and physics algorithms is resolved in such a way to ensure unequivocal results.

ACKNOWLEDGMENT

The authors would like to thank Gabriele Cosmo for valuable discussions concerning Geant4 geometry, Anita Hollier for proofreading the manuscript, and the Computing Service at INFN Genova for support regarding the computational infrastructure used in the tests.

REFERENCES

[1] S. H. Kim *et al.*, "Validation test of Geant4 simulation of electron backscattering," *IEEE Trans. Nucl. Sci.*, vol. 62, no. 2, pp. 451–479, Apr. 2015 [Online]. Available: http://arxiv.org/abs/1502.01507.

[2] S. Agostinelli *et al.*, "Geant4 - a simulation toolkit," *Nucl. Instrum. Methods Phys. Res. A*, vol. 506, no. 3, pp. 250–303, 2003.

[3] J. Allison *et al.*, "Geant4 developments and applications," *IEEE Trans. Nucl. Sci.*, vol. 53, no. 1, pp. 270–278, Feb.. 2006.

[4] L. Urban, "Multiple scattering model in Geant4," CERN-OPEN-2002-070, Geneva, Switzerland, 2002.

[5] L. Urban, "A model for multiple scattering in Geant4," The Monte Carlo Method: Versatility Unbounded in a Dynamic Computing World, CD-ROM, American Nuclear Society, La Grange Park, IL, USA, 2005.

[6] L. Urban, "A model of multiple scattering in Geant4," CERN-OPEN-2006-077, Geneva, Switzerland, 2006.

[7] S. Goudsmit and J. L. Saunderson, "Multiple scattering of electrons," *Phys. Rev.*, vol. 58, pp. 24–29, 1940.

[8] S. Goudsmit and J. L. Saunderson, "Multiple scattering of electrons. II," *Phys. Rev.*, vol. 58, pp. 36–42, 1940.

[9] O. Kadri, V. Ivanchenkob, F. Gharbi, and A. Trabelsi, "Incorporation of the Goudsmit-Saunderson electron transport theory in the Geant4 Monte Carlo code," *Nucl. Instrum. Methods Phys. Res. B*, vol. 267, no. 23–24, pp. 3624–3632, 2009.

[10] G. Wentzel, "Zwei bemerkungen uber die zerstreuung korpuskularer strahlen als beugungserscheinung," *Z. Physik*, vol. 40, no. 8, pp. 590–593, 1926.

[11] V. N. Ivanchenko *et al., J. Phys. Conf. Ser.*, vol. 219, p. 032045, 2010.

[12] J. Apostolakis *et al.*, "The performance of the Geant4 standard EM package for LHC and other applications," *J. Phys. Conf. Ser.*, vol. 119, p. 032004, 2008.

[13] V. N. Ivanchenko, M. Maire, and L. Urban, "Geant4 standard electromagnetic package for HEP applications," in *Proc. IEEE Nuclear Science Symp. Conf. Rec.*, 2004, pp. N33–179.

[14] J. Apostolakis, S. Giani, M. Maire, P. Nieminen, M. G. Pia, and L. Urban, "Geant4 low energy electromagnetic models for electrons and photons," INFN/AE-99/18, Frascati, Italy, 1999.

[15] S. Chauvie, G. Depaola, V. Ivanchenko, F. Longo, P. Nieminen, and M. G. Pia, "Geant4 low energy electromagnetic physics," in *Proc. Int. Conf. Computing in High Energy and Nuclear Physics*, Beijing, China, 2001, pp. 337–340.

[16] S. Chauvie *et al.*, "Geant4 low energy electromagnetic physics," in *Proc. IEEE Nuclear Science Symp. Conf. Rec.*, 2004, pp. 1881–1885.

[17] Geant4 10.1, "User's guide: For application developers," [Online]. Available: http://geant4.web.cern.ch/geant4/UserDocumentation/UsersGuides/ForApplicationDeveloper/html/index.html

[18] S. T. Perkins, D. E. Cullen, and S. M. Seltzer, "Tables and graphs of electron-interaction cross sections from 10 eV to 100 GeV Derived from the LLNL Evaluated Electron Data Library (EEDL)," UCRL-50400, vol. 31, 1997.

[19] D. Cullen *et al.*, EPDL97, The Evaluated Photon Data Library, Lawrence Livermore National Laboratory, Rep. UCRL-50400, 1997, vol. 6, Rev. 5.

[20] T. W. Anderson and D. A. Darling, "Asymptotic theory of certain goodness of fit criteria based on stochastic processes," *Ann. Math. Stat.*, vol. 23, pp. 193–212, 1952.

[21] T. W. Anderson and D. A. Darling, "A test of goodness of fit," *J. Amer. Stat. Ass.*, vol. 49, pp. 765–769, 1954.

[22] H. Cramér, "On the composition of elementary errors. Second paper: Statistical applications," *Skand. Aktuarietidskr*, vol. 11, pp. 13–74–141–180, 1928.

[23] R. von Mises, *Wahrscheinlichkeitsrechnung und ihre Anwendung in der Statistik und theoretischen Physik*. Leipzig, Germany: F. Duticke, 1931.

[24] A. N. Kolmogorov, "Sulla determinazione empirica di una legge di distribuzione," *Gior. Ist. Ital. Attuari*, vol. 4, pp. 83–91, 1933.

[25] N. V. Smirnov, "On the estimation of the discrepancy between empirical curves of distributions for two independent samples," *Bull. Math.*, 1939, Moscow Univ.

[26] G. S. Watson, "Goodness-of-fit tests on a circle," *Biometrika*, vol. 48, pp. 109–114, 1961.

[27] G. A. P. Cirrone *et al.*, "A goodness-of-fit statistical toolkit," *IEEE Trans. Nucl. Sci.*, vol. 51, no. 5, pp. 2056–2063, Oct. 2004.

[28] B. Mascialino, A. Pfeiffer, M. G. Pia, A. Ribon, and P. Viarengo, "New developments of the goodness-of-fit statistical toolkit," *IEEE Trans. Nucl. Sci.*, vol. 53, no. 6, pp. 3834–3841, Dec. 2006.

[29] R Core Team, "R: A language and environment for statistical computing," R Foundation for Statistical Computing, Vienna, Austria, 2012 [Online]. Available: http://www.R-project.org/, ISSN 3-900051-07-0

[30] G. Cosmo, "The Geant4 geometry modeler," in *Proc. IEEE Nuclear Science Symp. Conf. Rec.*, 2004, pp. 2196–2198.

[31] T. Basaglia *et al.*, bssim: Bssim-v2.0, 2015 [Online]. Available: http://dx.doi.org/10.5281/zenodo.18169

[32] T. Wenaus *et al.*, GEANT4: An Object-Oriented Toolkit for Simulation in HEP, Geneva, Switzerland, CERN-LHCC-97-040 Rep., 1997.

[33] S. Giani, GEANT4: An Object-Oriented Toolkit for Simulation in HEP, Geneva, Switzerland, CERN-LHCC-98-044 Rep., 1998.

[34] G. Cosmo, "Geant4 towards major release 10," *J. Phys. Conf. Ser.*, vol. 513, p. 022005, 2014.

[35] E. Juergens, F. Deissenboeck, B. Hummel, and S. Wagner, "Do code clones matter," in *Proc. 31st IEEE Computer Society Int. Conf. Software Engineering*, Washington, DC, USA, 2009, pp. 485–495.